Proc. Natl. Acad. Sci. USA
Vol. 83, pp. 2777–2781, May 1986
Astronomy

Ultraviolet spectrum and probable chemical composition of the high-excitation planetary nebula M1-1

(gaseous nebula/nucleogenesis/stellar evolution)

LAWRENCE H. ALLER†, CHARLES D. KEYES†, AND WALTER A. FEIBELMAN‡

†Astronomy Department, University of California, Los Angeles, CA 90024; and ‡National Aeronautics and Space Administration, Laboratory for Astronomy and Solar Physics, Goddard Space Flight Center, Greenbelt, MD 20771

Contributed by Lawrence H. Aller, December 11, 1985

ABSTRACT **One of the highest excitation planetary nebulae known, M1-1, was studied with the image-tube scanner on the Shane 3-m telescope at Lick Observatory and with the International Ultraviolet Explorer. Large fractions of abundant elements such as C, N, O, S, and Ar exist in unobservable stages of ionization. Hence, it is difficult to establish the chemical composition of this nebula. The logarithmic abundance values of various elements compared with those of the Sun appear to be as follows:**

	He	C	N	O	Ne	S	Ar
M1-1	11.02	8.57	8.4	8.7	7.95	6.6:	6.32
Sun	11.0	8.66	7.98	8.91	8.05	7.2	6.57

Here log N(H) = 12. In contrast to NGC 6537, the composition of M1-1 does not appear to differ markedly from that of the Sun. N may be enhanced but there is no enhancement of He or C. In spite of its high excitation and its presumed origin from a relatively massive star, M1-1 shows no evidence for pronounced nuclear processing.

The planetary nebula M1-1, also designated as (130 − 11°1) and VV5, recently has been studied spectroscopically by Barker (1–3) and by Aller and Czyzak (4). Especially notable are the high intensities of [Ne V] λ3346, λ3426, and He II λ4686.

Table 1 summarizes some of the relevant data. We give the position as measured at radio frequencies with the very large array (VLA) (5). The object is compact and of moderate surface brightness. Fortunately, the measured flux at Hβ (1, 7) is attenuated only by about 7 decibels, rather a modest amount for a somewhat distant planetary nebula. Distance estimates (6, 11, 12) show a discouragingly large scatter. Barker (2) has suggested that M1-1 belongs to Population II, though it does not have a very high radial velocity. The expansion rate of 24 km/sec (13) is normal for a planetary nebula.

Spectrum

The spectrum of M1-1 has been measured by photographic photometry in the region λ3133–4959 (8), by photoelectric photometry (1), and with the image-tube scanner (ITS) at the Shane 3-m telescope (9). These latter measurements were made with the so-called red tube, and the coverage below λ4000 Å was poor. The new series of observations was made with the ITS with the so-called green tube, which is sensitive to λ3100 Å, and with the International Ultraviolet Explorer (IUE). Details are given in Table 2. The observational procedures with the ITS are described in ref. 4.

Before the data can be employed, they must be corrected for interstellar extinction. For a summary of some of the most popular methods see, for example, ref. 14, pp. 187–193. For the optical region data we have employed the Balmer decrement, but for the ultraviolet the best procedure is to employ the Paschen/Balmer ratio in He II or, more precisely, the ratio of λ4686(Pa α)/λ1640(Ba α). This ratio depends on the electron temperature, T_e, and only slightly on the electron density, N_e. Its functional dependence has been tabulated by Seaton (15). Since the angular size of M1-1 is smaller than the entrance slot in the IUE, we may compare directly the fluxes measured with those found in optical region photometry (1, 7). We evaluated the quantity $C = \log I(\mathrm{H}\beta)/F(\mathrm{H}\beta)$, where $F(\mathrm{H}\beta)$ is the measured flux in erg·cm^{-2}·sec^{-1} and $I(\mathrm{H}\beta)$ is the same corrected for interstellar extinction. The agreement between the two determinations is very good; we retain C = 0.67 in the reduction of optical region data in order to allow for possible effects arising from slight errors in atmospheric extinction or the response function of the detector.

Table 3 gives the measured intensities in the near-ultraviolet as obtained from the Lick Observatory ITS data. The first column gives the wavelength in Å, the second column the identification, and the third column the intensity on the scale $I(\mathrm{H}\beta)$ = 100. The intensity is corrected for interstellar extinction with the Seaton f_λ function (16) assuming C = 0.67. The fourth column gives the estimated error in the individual measurements (in percent) as estimated from the internal agreement of the individual measurements. It does not include any systematic effects, such as might arise from placement of the underlying continuum, or the effects of errors in the response function or assumed atmospheric extinction. On the basis of previous studies (17), we estimate that this error might amount to about 5% longward of 3250 but may amount to 10–20% in shorter wavelength regions. Fig. 1 shows a scan of the region λ1200–1950 as observed with the SWP camera of the IUE. Identifications of strongest lines are marked.

Table 4 lists the ultraviolet line intensities measured with the IUE. First we list the wavelength and identifications and then the measured fluxes in units of 10^{-12} erg·cm^{-2}·sec^{-1}. Figures enclosed in parentheses are uncertain. The fourth column gives f_λ, the interstellar extinction function given by Seaton (16). Then $\log I_\lambda = \log F_\lambda + Cf_\lambda$. The fifth column gives the intensity corrected for interstellar extinction and normalized to $I(\mathrm{H}\beta)$ = 100 using C = 0.70. Errors may be estimated by comparing independent measurements of the flux on scans SWP 17571 and 21420. Unfortunately, only a few lines are common to the two exposures. We found σ values of 20%, 30%, and 18% for λ1240, λ1487, and λ1750, respectively. For weak lines the errors are larger, of course.

Plasma Diagnostics and Ionic Concentrations

Two fundamental parameters for analyses of spectral data are the electron density N_e and electron temperature T_e. These parameters are generally called the plasma diagnostics. They are obtainable from the ratios of collisionally excited lines (see refs. 14, 18–20). Ratios of forbidden doublets in nebular-

Abbreviations: VLA, very large array; ITS, image-tube scanner; IUE, International Ultraviolet Explorer; ICF, ionization correction factor.

Table 1. Basic data for M1-1 (130 − 11°1) VV5

Position α = 01 hr 34 min 13.01 sec
δ = +50° 12′ 56.3″ } (1950) (ref. 5)
Angular diameter 6″ (ref. 6)
Logarithm of Hβ flux in erg·cm^{-2}·sec^{-1}
log $F(H\beta)$ = −11.88 (ref. 7)
= −11.94 (ref. 1)
Extinction constant C = log $F_c(H\beta)/F(HB)$, where $F_c(H\beta)$ is the flux corrected for interstellar extinction.
C = 1.47 $E(B - V)$, where the color excess is denoted by $E(B - V)$.
C = 0.53 (ref. 8); = 0.45 (ref. 9); = 0.33 ± 0.03 (ref. 1)
Radial velocity
(with respect to local standard of rest) V_{lsr} = −35.1 km/sec (ref. 10)
(heliocentric velocity) V_{hel} = −38 ± 1.8 km/sec (ref. 10)
Distance in parsecs (1 parsec = 3.09 × 10^{16} m)
5300 ± 700 (ref. 11); 2900 (ref. 6); ≤6100 (ref. 12)
Radio frequency flux in millijanskys (mJy)
(1 jansky = 10^{-26} W·m^{-2}·Hz^{-1})
(6 cm) = 8.6 mJy (ref. 5)
(20.5 cm) = 9.3 mJy (ref. 5)
Expansion velocity
2 V_{exp}([O III]) = 24.0 km/sec (ref. 13)
Excitation class 10 (ref. 8)

type transitions of the p^3 configuration—e.g., [S II], [O II]—are particularly sensitive to the electron density. Ratios of the auroral-type to nebular-type transitions in p^2 configurations depend primarily on T_e—e.g., [O III]. The auroral-type to nebular-type transitions in p^3 configurations—e.g., in [O II] and [Ne IV]—vary markedly with both T_e and N_e.

Fig. 2 shows the plasma diagnostics for M1-1. We plot the auroral/nebular (A/N) ratios for [O III] λ4363/4959 + 5007 and [O II] 3727/7325 and [Ne IV] 2424/4723, the nebular doublet ratio 3729/3726 [O II], and 6717/6730 [S II] as a function of electron temperature and density. The auroral/nebular line ratio in [O III] due to Barker yields the dashed line.

If the nebular plasma had a uniform temperature and density, all of these curves would intersect at a common point. Inspection of the diagram shows immediately that the [O II] and [S II] radiations originate primarily in strata at different densities, the S^+ ions predominating in the zone of higher N_e. Likewise, the [Ne IV] radiation originates in a hotter zone than does the [O II] or [O III] radiation, which is to be expected from elementary considerations. The [O II] and [O III] curves intersect near a point, so we adopted T_e = 15,800 K, log N_e = 3.30 for most ions. Exceptions are [S II] for which we assume log N_e = 3.60 and [Ne IV] and other high-excitation ions for which we must use temperatures in excess of 16,000 K. Here we rely on theoretical nebular models.

The first five columns of Table 5 give for each ion the lines used in the analysis, the intensities of the lines as corrected for interstellar extinction, which come from data in Tables 3 and 4 and ref. 4, values of $t = T_e/10{,}000$, and $N(X_i)$ in units of $N(H^+)$—that is, the concentration of each type of ion in terms of hydrogen ions.

Table 2. List of observations

	Spectral region, Å	Total dwell time, min	Date
ITS (Lick 3-m telescope)	3100–4000	80	Nov. 12, 1979
IUE			
SWP 17571	1200–1950	70	Aug. 2, 1982
LWR 13850	1900–3210	80	Aug. 2, 1982
SWP 21240	1200–1950	165	Aug. 31, 1983

Ionic concentrations for He^+ and He^{2+} are derived from the recombination lines of He I and He II, respectively. Appropriate equations have been given—e.g., by Barker (2). At the densities with which we are concerned, these concentration ratios depend only on T_e.

For collisionally excited lines, relevant equations have been given by many workers (e.g., refs. 14, 18–20). Alternatively, one can use programs to solve the relevant equations of statistical equilibrium and compute $N(X_i)/N(H^+)$ as a function of $N(X_i)/I(H\beta)$. Mendoza (21) has given a useful compilation of atomic data up to 1982.

The accuracy of the derived values of $N(X_i)$ can be no better than that of the input data. The role of the electron temperature is very important. For lines in the ultraviolet, especially, small errors in T_e can lead to large errors in the derived $N(X_i)$. The auroral/nebular ratio in [Ne IV] (see Fig. 2) suggests $T_e \approx 17{,}500$ in the zone where this line originates. The model can be of some help here. The uncertainty is large because I(λ4725) is not determined with high accuracy and I(λ2424) can be in error by the order of 10–20%. Thus, for these high-excitation regions we have to rely on theoretical models for realistic temperature estimates. The [Mg V] and [Si III] data are so uncertain that we have not tried to estimate the abundances of these elements.

The sum of the concentrations of the observed ions, $\Sigma N(X_i)$, is given in column 6 of Table 5. Our next task is to obtain the elemental abundances, $N(el)$, in terms of hydrogen.

Determination of the Nebular Chemical Composition

The fundamental question is to determine the ionization correction factor (ICF) whereby we may obtain the total number of atoms in all stages of ionization from the number in observed stages of ionization. This task poses no difficulty for helium in moderate-to-high-excitation nebulae, for virtually all He atoms exist as He^+ or He^{2+} ions. For other atoms, one frequently uses empirical formulae (see, e.g., ref. 14, p. 249, for a compilation). Such formulae seem to work reasonably well for nitrogen in most nebulae, as has been demonstrated by the work of Barker (22), for example. For neon the situation is less clear, whereas for sulfur, chlorine, and argon, these empirical formulae are of questionable usefulness. Nebulae of extremely high excitation pose particular difficulties.

Table 3. Spectrum of M1-1 (130 − 11°1) in the region λ3100–3950 Å

λ, Å	Identification	*I*	σ (%)	λ, Å	Identification	*I*	σ (%)
3132.9	O III	32	20	3692	H18	0.77	(30)
3187.8	He I	3.0	25	3698	H17	0.90	14
3203.1	He I	44	15	3705	H16 + H17	1.41	(15)
3242	[Na IV]	1.4	50	3713	H15	1.54	(15)
3299	O III	0.69	29	3722	H15, [S III]	2.42	20
3312	O III	2.0	16	3726	[O II]	17.6	19
3317	Fe III	0.9	30	3729	[O II]	11.6	
3340.8	O III	3.1	12	3734	H13	2.8	18
3345.9	[Ne V]	99	3	3750	H12	3.17	(10)
3362	[Na IV]	0.97	7	3754	O III	0.85	(13)
3381.2	O IV	1.3	(22)	3760	O III	2.14	14
3385.5	O IV	0.94	(18)	3770.6	H II	4.17	(3)
3398	O IV	0.64	(20)	3781	He II	0.37	29
3411.7	O IV	0.91	(40)	3791.2	O III	0.22	20
3426.0	[Ne V]	289	5	3797.8	H10	5.14	(5)
3444	O III	5.9	11	3813	He II	0.54	31
3554	He I	0.6	50	3819.6	He I	0.29	33
3566		0.6	50	3835.3	H9	7.9	(5)
3587	He I	0.24	50	3858.1	He II	0.87	18
3634	He I	0.58	15	3868.8	[Ne III]	36	4
3683	H20	0.35	30	3888.9	H8, He I	14.1	3
3687	H19	0.68	20	3923.5	He II	0.91	10

I = intensity corrected for interstellar extinction with Seaton (16) extinction coefficient and $C = 0.67$.

Ideally, one would like to obtain a model that would reproduce the observed spectrum. This is a necessary but not a sufficient condition. It is possible to obtain two quite different models that reproduce the line intensities equally well (or equally badly) and from which we would derive different ICFs. There are two very substantial reasons why it is often impossible to obtain a satisfactory theoretical model for a real nebula. (*i*) Theoretical models are spherically symmetrical, usually, with the density a function of *r*, the distance from the central star. It is possible to put in perturbations in the form of denser blobs, etc., or by the use of a nonuniform shell with tessera of different densities. Real nebulae often have significant irregularities and "condensations" that are almost impossible to model in any meaningful way. (*ii*) The energy distribution in the central star $F_\nu(*)$ is not known. For effective temperatures below about 120,000 K, plausible stellar fluxes are available. For higher levels of excitation we often start with blackbodies, but we find that these flux distributions have to be modified.

It became clear early in our attempted modeling of M1-1 that none of the published theoretical stellar energy fluxes would be satisfactory, so we tried using a higher temperature blackbody energy distribution. The extreme strength of [Ne V] presents a unique problem. Early attempts (9) to construct nebular models in the absence of far-ultraviolet data were unsatisfactory. Only with the advent of IUE data was it possible to address the problem more directly.

Spherical nebular models with central stars radiating as blackbodies with temperatures as high as 225,000 K would not work and shell models were even less satisfactory. We modified the 180,000 K Planckian flux in the region 7.25–9.05 Rydberg (1 Rydberg = 3.25×10^{15} Hz), raising it there by about a factor of 2. The procedure amounted somewhat to putting in a hot wind above an extended photosphere, but its *ad hoc* nature cannot be evaded. The distribution of atoms of various elements among different stages of ionization simply could not be reproduced by an input stellar Planckian distribution. This model did lead to a theoretical spectrum

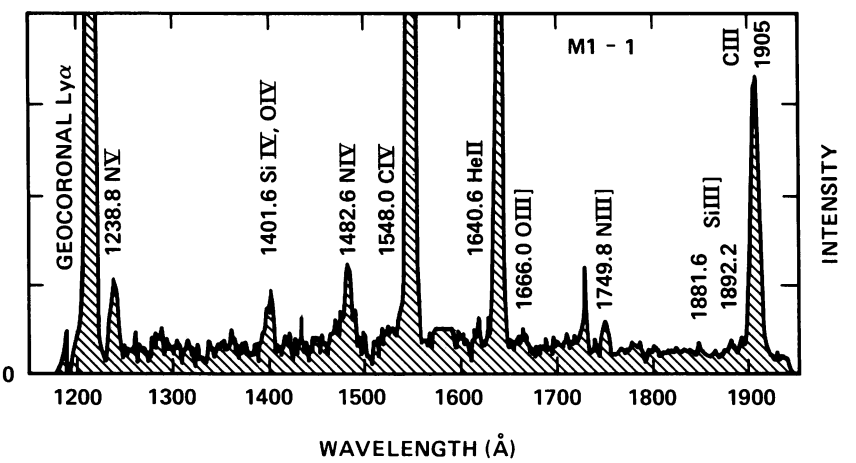

FIG. 1. The λ1200–λ1950 region of M1-1 as observed with the IUE SWP camera. This 165-min exposure (scan 21240) was intended to bring out the weaker features. Hence, strong emissions such as λ1548 and λ1640 are saturated (i.e., burned out). The flat-topped interval near λ1590 indicates the region of a noise spike that is not plotted.

Table 4. Ultraviolet spectrum of M1-1 (130 − 11°1)

λ, Å	Identification	$F \times 10^{12}$	f_λ	I
1240	N V	0.35	1.641	416
1401	Si IV, O IV	0.276	1.308	194
1487	N IV	0.43	1.231	267
1548, 1550	C IV	3.15	1.185	1820
1575	Ne V	0.12	1.169	67.5
1640	He I	1.32	1.138	706
1750	N III	0.14	1.121	73
1881	Si III	(0.033)	1.200	(19)
1892	Si III	(0.046)	1.208	(27)
1906, 1909	C III	0.93	1.228	575
2424	[Ne IV]	0.41	1.122	214
2929	Mg V	(0.08)	0.56	(17)
3081		(0.26)	0.48	(48)
3133	O III	(0.08)	0.458	(14)

that generally fitted the [Ne V] lines and the ultraviolet lines observed with the IUE, including [Ne IV], although it did not predict sufficiently strong *N* V λ1238. A more serious problem was that it did not reproduce the lines of [N II] λ6583 and [Ne III] λ3868. In fact, these emissions were predicted much too strong, although [O II] and [O III] were predicted about right. If we had chosen abundances to fit only the optical region [N II] and [Ne III] lines, we would have been in error by a factor of 3 or more in predicting the ultraviolet nitrogen and neon ionic lines.

Thus, if we use this model to predict ICFs for N, Ne, and possibly C using the $\Sigma N(X_i)$ in column 6 of Table 5, we probably come out with reasonable results. The model fits the data for higher stages of ionization observed with the IUE and can probably be trusted for extrapolating for unobserved ionization stages. For oxygen there seems to be serious trouble. Lines of O IV and O V are not observable in this object. The ICF factor of about 2.5 for $N(O^+) + N(O^{2+})$ leads to an oxygen abundance that looks implausibly low. One procedure might be to go to inhomogeneous models of somewhat complex structure, but the uncertainty imposed by the unknown $F_\nu(*)$ would remain. Instead, we noted that the distribution of neon ions among higher ionization stages was fairly well defined, and if the vast bulk of neon atoms were in

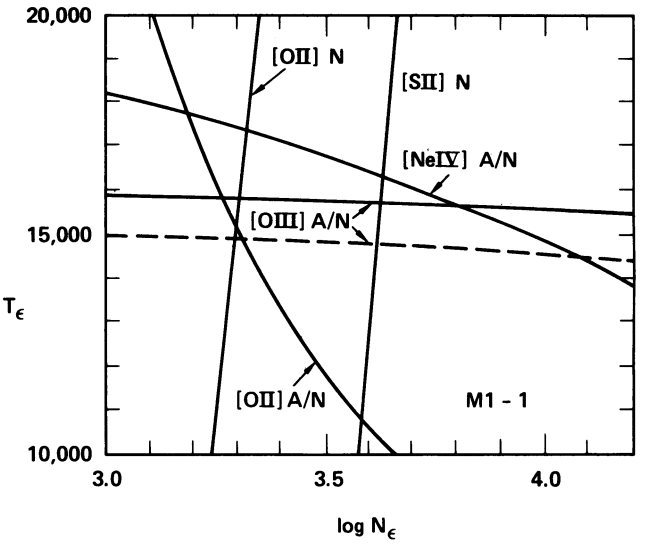

FIG. 2. Plasma diagnostics for M1-1 (see text).

stages of ionization higher than Ne^{2+}, the same would be true for oxygen. We postulated $N(Ne)/N(Ne^{2+}) \cong N(O)/N(O^{2+})$.

Column 7 in Table 5 gives the adopted ICFs. We have taken them from the theoretical model for ions represented by higher stages of ionization, but for oxygen we have used an ICF of 11, obtained by the aforementioned argument. By similar reasoning, it is clear that we can derive no satisfactory result for sulfur, only a lower limit.

Discussion

Table 6 compares data for M1-1, NGC 6302, NGC 6537, NGC 6741 (23–25), the "mean" value for a sample of planetary nebulae (9), and the Sun (26). In Table 6 we confine our comparisons to nebulae observed with similar equipment and analyzed by the same ICF model methods.

If we compare M1-1 with the mean planetaries, we note that the abundances do not differ by more than about a factor of 2. Similar remarks hold rather well for the solar abundances. The nitrogen-rich nebulae NGC 6537 and NGC 6302

Table 5. Estimation of elemental abundances in M1-1

Ion	λ, Å	I	t	$N(X_i)$	$\Sigma N(X_i)$	ICF	$N(el)$
He I	5876	1.89	1.58	0.016	0.106	1.0	0.107
	4471	0.57					
He II	4686	101	1.58	0.090			
C III	1909	578	1.58	7.84 (−5)	1.74 (−4)	2.1	3.7 (−4)
C IV	1549	1820	1.68	9.60 (−5)			
N II	6583	13.1	1.58	9.4 (−7)			
N III	1750	73	1.58	4.1 (−5)	1.84 (−4)	1.35	2.5 (−4)
N IV	1487	267	1.68	9.3 (−5)			
N V	1240	416	1.85	4.9 (−5)			
O II	3727	29.2	1.58	2.9 (−6)	5.05 (−5)	11:	5: (−4)
O III	4959, 5007	593	1.58	4.76 (−5)			
Ne III	3868	36	1.58	7.5 (−6)			
Ne IV	2424	214	1.66	3.2 (−5)	7.9 (−5)	1.12	8.9 (−5)
Ne V	3345, 3426	388	1.80	4.0 (−5)			
Na IV	3242, 3362	2.37	1.58	6.2 (−7):		5.4	3.3 (−6)
Si III	1892	27.3	1.58	8.2 (−7)			
S II	6717, 6730	2.3	1.58*	3.9 (−8)	7.4 (−7)	>5	>4 (−6)
S III	6312	1.46	1.58	7.0 (−7)			
Ar III	7135	4.8	1.58	1.65 (−7)			
Ar IV	4740	5.2	1.58	6.2 (−7)	1.0 (−6)	2.1	2.1 (−6)
Ar V	6435, 7005	6.4	1.61	2.15 (−7)			

*For [S II] we assume $N_e = 4000$. In this and other tables a colon (:) after a figure indicates it is uncertain.

Table 6. Comparison of elemental abundances; log $\{N(el)/N(H)\} + 12.00$

Element	Present M1-1	NGC 6302	NGC 6537	NGC 6741	"Mean" PN	Solar
He	11.025	11.26	11.27	11.037	11.04	
C	8.57	8.00	7.56	9.08	8.89	8.66
N	8.40	8.92	8.94	8.72	8.26	7.98
O	8.7:	8.70	8.19	8.73	8.64	8.91
Ne	7.95	7.99	7.98	8.20	8.03	8.05
Na	6.5:	6.57		6.5	6.18	6.31
S	6.6:	6.8	7.13	6.99	7.00	7.23
Ar	6.32	6.93	6.73	6.56	6.43	6.57

PN, planetary nebulae. (:) Uncertain values.

also have strong excesses of helium, whereas the He abundance in M1-1 is essentially normal. For neon and beyond, the abundance pattern seems to be similar in all objects. NGC 6537 and NGC 6302 show large effects of nuclear processing in C, N, and possibly O, whereas, M1-1, in spite of the high excitation of its spectrum, shows rather insignificant effects of nuclear processing.

Simple theoretical models, at least, can fail for nebulae of such high excitation as M1-1, but such models may be useful in providing clues to the electron temperatures in the hotter zones, where the auroral/nebular ratio in [Ne IV] gives helpful clues. In particular, the models cannot give much help in supplying ICFs for an element such as S, which has no high ionization stage represented in the ultraviolet. Another complicating factor is the influence of possible temperature fluctuations. Corrections for these effects would enhance the computed abundances of elements represented by collisionally excited lines (27, 28). We need to push to the very limit of the far-ultraviolet window near the Lyman limit and into the infrared to obtain data on ions such as O IV and O VI. The critical value of IUE data is well demonstrated in this investigation.

We are grateful to the staffs and technical experts at Lick Observatory and Goddard Space Flight Center for assistance in obtaining the observations. We also appreciate the careful typing of the manuscript by Mr. Robert L. O'Daniel. This program was supported in part by National Science Foundation Grant AST 83-12384 to the University of California, Los Angeles. We are also indebted to the National Aeronautics and Space Administration for Grant NSG 5358 to support IUE observations and attempts at theoretical models.

1. Barker, T. (1978) *Astrophys. J.* **219,** 914–930.
2. Barker, T. (1978) *Astrophys. J.* **220,** 193–209.
3. Barker, T. (1978) *Astrophys. J.* **221,** 145–150.
4. Aller, L. H. & Czyzak, S. J. (1979) *Astrophys. Space Sci.* **62,** 387–413.
5. Isaacman, R. (1984) *Mon. Not. R. Astron. Soc.* **208,** 399–408.
6. Daub, C. T. (1982) *Astrophys. J.* **260,** 612–624.
7. Carrasco, L., Serrano, A. & Costero, R. (1983) *Rev. Mex. Astron. Astrofis.* **8,** 187–192.
8. Kaler, J. B., Aller, L. H. & Czyzak, S. J. (1976) *Astrophys. J.* **203,** 636–646.
9. Aller, L. H. & Czyzak, S. J. (1983) *Astrophys. J. Suppl.* **51,** 211–248.
10. Schneider, S. E., Terzian, Y., Purgathofer, A. & Perinotto, M. (1983) *Astrophys. J. Suppl.* **52,** 399–423.
11. Acker, A. (1978) *Astron. Astrophys. Suppl.* **33,** 367–379.
12. Maciel, W. J. (1984) *Astron. Astrophys. Suppl. Ser.* **55,** 253–258.
13. Sabbadin, F. (1984) *Astron. Astrophys. Suppl. Ser.* **58,** 273–285.
14. Aller, L. H. (1984) *Physics of Thermal Gaseous Nebulae* (Reidel, Dordrecht, The Netherlands).
15. Seaton, M. J. (1978) *Mon. Not. R. Astron. Soc.* **185,** 5P–8P.
16. Seaton, M. J. (1979) *Mon. Not. R. Astron. Soc.* **187,** 73P–76P.
17. Likkel, L. J. & Aller, L. H. (1986) *Astrophys. J.*, in press.
18. Seaton, M. J. (1960) *Rep. Prog. Phys.* **23,** 313–354.
19. Osterbrock, D. E. (1974) *Astrophysics of Gaseous Nebulae* (Freeman, San Francisco).
20. Aller, L. H. & Liller, W. (1968) in *Stellar Systems*, eds. Middlehurst, B. & Aller, L. H. (University of Chicago Press, Chicago), Vol. 7, 483–574.
21. Mendoza, C. (1983) in *Planetary Nebula*, International Astronomical Union Symposium No. 105, ed. Flower, D. R. (Reidel, Dordrecht, The Netherlands), pp. 143–172.
22. Barker, T. (1981) *Astrophys. J.* **240,** 99–104.
23. Aller, L. H., Ross, J. E., O'Mara, B. J. & Keyes, C. D. (1981) *Mon. Not. R. Astron. Soc.* **197,** 95–106.
24. Feibelman, W., Aller, L. H., Keyes, C. D. & Czyzak, S. J. (1985) *Proc. Natl. Acad. Sci. USA* **82,** 2202–2206.
25. Aller, L. H., Keyes, C. D. & Czyzak, S. J. (1985) *Astrophys. J.* **296,** 492–501.
26. Aller, L. H. (1986) in *Spectroscopy of Astrophysical Plasmas*, eds. Dalgarno, A. & Layzer, D. (Cambridge University Press, Cambridge, U.K.).
27. Peimbert, M. (1967) *Astrophys. J.* **150,** 825–834.
28. Rubin, R. H. (1969) *Astrophys. J.* **155,** 841–851.